https://rbgeomorfologia.org.br/
ISSN 2236-5664

Revista Brasileira de Geomorfologia

v. 26, nº 4 (2025)

https://dx.doi.org/10.20502/rbg.v26i4.2635

Research paper

Analysis of the coastal vulnerability index to erosion and flooding in the Porto Seguro (BA) region and surrounding areas

Vulnerabilidade costeira à erosão e inundação da região de Porto Seguro (BA) e adjacências

Gabriela Nunes Rebouças Leal [1], Catarina da Rocha Marcolin [2] e Tatiana Pinheiro Dadalto [3]

[1] Federal University of Southern Bahia / Federal Institute of Science and Technology of Bahia, Graduate Program in Environmental Science and Technology, Porto Seguro, Brazil. E-mail: gabrielanunesleal@gmail.com
ORCID: https://orcid.org/0009-0005-0268-1852

[2] Federal University of Southern Bahia / Federal Institute of Science and Technology of Bahia, Graduate Program in Environmental Science and Technology, Porto Seguro, Brazil. E-mail: catarina.marcolin@gfe.ufsb.edu.br
ORCID: https://orcid.org/0000-0003-3701-3772

[3] Federal University of Southern Bahia, Center for Environmental Science Education, Porto Seguro, Brazil. E-mail: tatiana.dadalto@gfe.ufsb.edu.br
ORCID: https://orcid.org/0000-0001-7823-8877

Received: 19/11/2024; Accepted: 30/09/2025; Published: 24/11/2025

Abstract: The coastal zone is a dynamic and complex environment with a diversity of ecosystems of significant economic importance. These factors increase real estate speculation in such areas, requiring efficiency in the management of natural and socioeconomic resources. The objective of this study was to estimate and analyze the Coastal Vulnerability Index (CVI) along a 25 km stretch of coastline between the municipalities of Porto Seguro and Santa Cruz Cabrália (Bahia, Brazil), taking into account physical, environmental, and socioeconomic factors. A total of 11 indicators were assessed, and the CVI was calculated for both moderate (MS) and pessimistic (PS) scenarios, considering constant and rising sea levels (CSL and RSL), using the AHP weighting technique. Our results indicated that under the moderate scenario with constant sea level (CSL-MS), 12.90% of the coast had low vulnerability, 59.77% moderate vulnerability, and 27.33% high vulnerability. In contrast, under the pessimistic scenario (CSL-PS), 80.95% of the coast showed high vulnerability. When considering the scenario of eustatic sea level rise (RSL-MS), 35.78% of the coast was classified as highly vulnerable, whereas in the pessimistic scenario (RSL-PS), this estimate rose to 98.48%. The Ponta Grande and Orla Norte beaches showed high vulnerability because of the presence of river mouths, and should be prioritized for conservation and adaptation efforts. The information provided here is essential for coastal planning and management in the region.

Keywords: geoprocessing, remote sensing, coastal environments, coastal management, southern Bahia.

Resumo: A zona costeira constitui um ambiente dinâmico e complexo, com diversidade de ecossistemas, de relevada importância econômica. Tais fatores elevam a especulação imobiliária nessas áreas, exigindo eficiência na gestão dos recursos naturais e socioeconômicos. O objetivo foi estimar e analisar o índice de vulnerabilidade costeira (IVC) em 25 km de costa entre os municípios de Porto Seguro e Santa Cruz Cabrália (BA), considerando fatores físicos, ambientais e socioeconômicos. Assim, foram avaliados 11 indicadores e o cálculo do IVC abrangeu cenários moderado (CM) e pessimista (CP) em relação ao nível do mar constante e elevado (NMC e ENM), utilizando a técnica de ponderação AHP. Os resultados indicaram que, no cenário moderado (NMC-CM), 12,90% da costa apresentaram baixa vulnerabilidade, 59,77% moderada e 27,33% alta. Em contraponto, no cenário pessimista (NMC-CP), 80,95% da costa demonstrou alta vulnerabilidade. Ao considerar o cenário de elevação eustática do nível do mar (ENM-CM), 35,78% mostrou alta vulnerabilidade, enquanto que no pessimista (ENM-CP), esse índice subiu para 98,48%. As praias da Ponta Grande e Orla Norte, junto às desembocaduras dos rios, apresentaram alta

vulnerabilidade e devem ser priorizadas para conservação e adaptação. As informações obtidas são fundamentais para o planejamento do uso e gestão da costa na região.

Palavras-chave: geoprocessamento, sensoriamento remoto, ambientes costeiros, gestão costeira, sul da Bahia.

1. Introduction

The coastal zone is a dynamic and complex environment, where the transition and interaction between air, ocean, and land take place (Rueda et al., 2017; Gracia Prieto, 2022). Due to its strategic location, wide diversity of ecosystems, and economic potential, this region has experienced a significant and disorderly population growth. It is estimated that 60% of the world's cities with more than 5 million inhabitants are located within 100 km of the coastline (Firth et al., 2016). In Brazil, approximately 50% of the population lives within 150 km of the coast (IBGE, 2022).

Such factors place pressure on this environment, especially in a context of climate change, where the increase in frequency and intensity of extreme events makes this area more vulnerable, exposing ecosystems and populations to erosion and flooding processes (Amaro et al., 2021). Rueda et al. (2017) found that 75% of the world's coastal zones have flood potential. Luijendijk et al. (2018) studied the world's sandy beaches from 1984 to 2016, identified that 24% of them are undergoing erosion at a rate greater than 0.5 m/year, 28% are accreting, and 48% remain stable. Mentaschi et al. (2018), in a global assessment of coastal morphodynamics over 32 years (1984–2015), indicated that 28,000 km² of coastline is eroding, while 14,000 km² is accreting.

In this context, understanding the interactions between natural and anthropogenic factors becomes necessary in order to promote better management of environmental resources. Serafim and Bonetti (2017) consider it strategic to develop tools capable of predictively assessing coastal exposure. The methods applied may vary depending on the need to address the specificities of the study area (Busman et al., 2016; Zanetti, Souza Jr.; Freitas, 2016). However, the lack of long-term monitoring data in coastal areas is a challenge, making scientific efforts in this direction particularly relevant.

Therefore, studies focused on assessing coastal vulnerability through indices based on metrics that integrate environmental and socioeconomic variables have increasingly been conducted in recent years (Aboudha and Woodroffe, 2010 in southeastern Australia; Pantusa et al., 2018 in Italy; Baig et al., 2020 in India; Zanetti, Souza Jr., and Freitas, 2016 in Santos, SP; Serafim and Bonetti, 2017 in Santa Catarina; Figueiras and Albino, 2020 in Espírito Santo; Carvalho and Guerra, 2020 on beaches in Rio de Janeiro; Queiroz, Gonçalves, and Mishra, 2022 in Pernambuco; Gouvea Jr., Fernandes, and Castro, 2022 in the Região dos Lagos – RJ).

In the northeastern coast of Brazil, the municipalities of Porto Seguro and Santa Cruz Cabrália stand out as major national tourist destinations. Silva et al. (2007) and Fernandino et al. (2019) identified beaches in this region with high erosive sensitivity and potential economic damage. In some locations, damage to roads can be observed, as well as the exposure of roots and retaining walls. Both municipalities feature sandy beaches with coral reefs, beachrocks, cliffs, mangroves, and estuaries, with dense development of large-scale enterprises such as hotels and beach bars.

This study aims to estimate and assess the Coastal Vulnerability Index in a section of the coastline of the municipalities of Porto Seguro and Santa Cruz Cabrália, using indicators and scenarios that reflect local characteristics and provide data on the most vulnerable coastal sectors, thus supporting the management of mitigation strategies and adaptation decisions in response to coastal disturbances, especially those related to climate.

2. Study Area

The study area covers approximately 25 km of coastline within the municipalities of Santa Cruz Cabrália (SCC) and Porto Seguro (PS), in the state of Bahia, Brazil (Figure 1). This coastal stretch includes 18 beaches, with four located in SCC (Arakakaí, Lençóis, Mutari, and Coroa Vermelha), seven along the northern shoreline of PS (Mutá, Ponta Grande, Taperapuã, Mundaí, Itacimirim, Curuípe, and Cruzeiro/Pitangueiras), and six in the district of Arraial D'Ajuda (Apaga Fogo, Araçaípe, Pescadores, Mucugê, Parracho, and Lagoa Azul).

The population of the municipality of Porto Seguro is 168,326 inhabitants, and that of Santa Cruz Cabrália is 30,862 (IBGE, 2022), reflecting an increase of approximately 33% in Porto Seguro and 11% in Santa Cruz Cabrália from 2010 to 2022. The coastline is characterized by the presence of coastal coral reefs located on the beaches of

Ponta Grande (PS), Mutá (PS), and Coroa Vermelha (SCC), as well as beachrocks associated with the mouths of the Buranhém River (PS) and João de Tiba River (SCC), along with abrasion terraces. The Atlantic Forest biome predominates in the region, with highly relevant environmental features such as beaches, estuaries, coastal sandbanks (*restingas*), *mussunungas*, wetlands, mangroves, and alluvial forests (Carvalho, Pimenta; Schiavetti, 2018). This stretch also includes river mouths.

The climate is classified as Af (hot and humid), according to the Köppen classification, with an average temperature of 24°C. The tidal regime is semidiurnal and ranges from microtidal (< 2 m) to mesotidal, with amplitudes above 2 meters during spring tides and/or frontal systems. According to Silva (2008), during autumn and winter, prevailing winds and waves come from the east (E) and southeast (SE), while in spring and summer, northeasterly (NE) winds are more frequent.

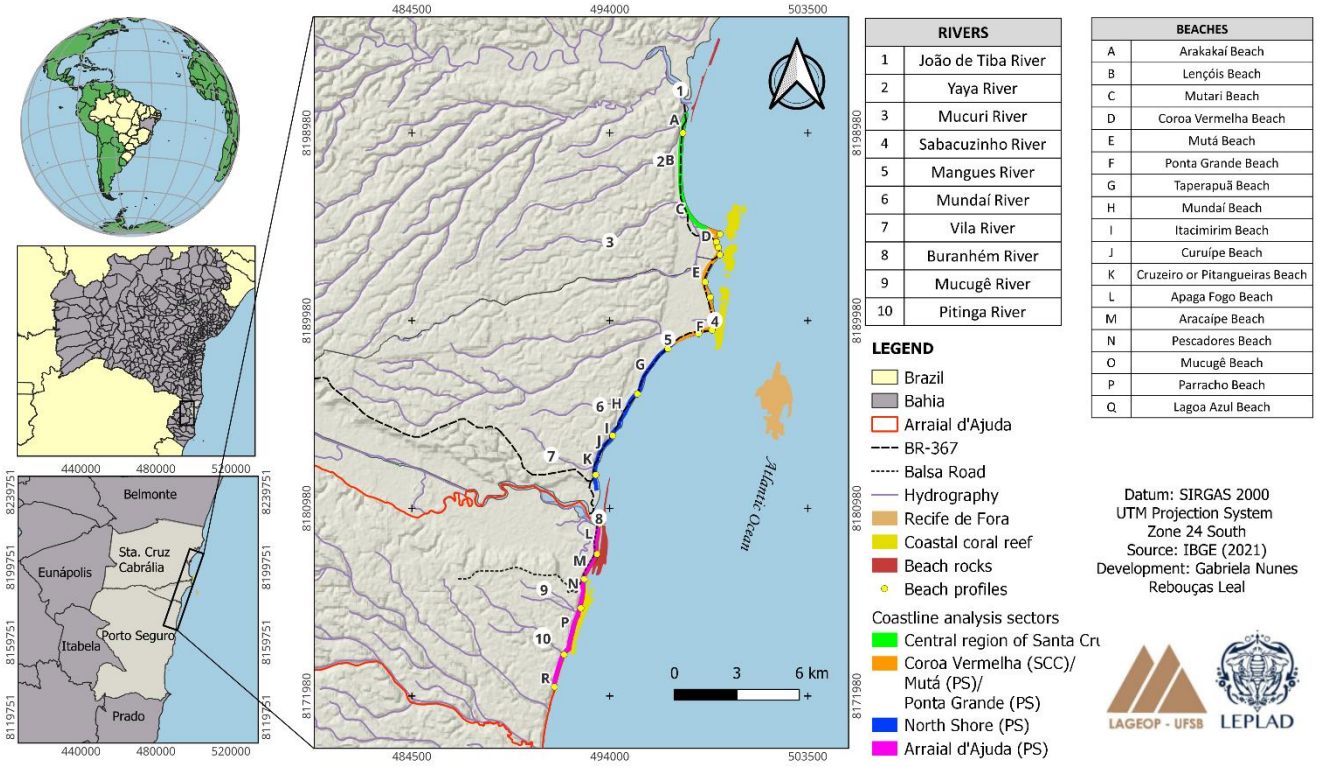

Figure 1. Study Area

3. Materials and Methods

Approximately 20 articles were selected with the aim of examining which indicators were assessed and how the authors calculated the Coastal Vulnerability Index. Following this stage, a survey of the socioeconomic and environmental data available for the study area was carried out. Subsequently, the feasibility of using these data in the construction of the index was evaluated, and data that could potentially be generated were identified.

In the following, eleven indicators were selected based on the characteristics of the study region, as well as the availability of the data found. Evaluation criteria were assigned to these indicators for the Coastal Vulnerability Index, taking into account the environmental characteristics and coastal dynamics of the study area, with reference to the works of Gornitz (1991), Bush et al. (1999), Sousa, Siegle and Tessler (2013), and Carvalho and Guerra (2020). Three vulnerability classes were applied: (1) low, (2) moderate, and (3) high. The data collection method for these indicators is described below.

3.1. Data Collection

- Rate of coastline change (m/year)

Historical images from Google Earth Pro were used, selected based on program availability, with the conditions of good resolution and no or low cloud cover. The temporal coverage spanned 18 years (2006 to 2023). The images were georeferenced in the QGIS GIS environment, version 3.28.8, using 10 predefined control points.

The most suitable coastline used was the vegetation line (Boak; Turner, 2005), as well as roads, paved areas, beach bars, and walls. Coastline extraction was performed by creating vector line files for each selected image, which were then merged into a single file. Using the Digital Shoreline Analysis System (DSAS/ArcMap) version 5.1, the coastline change rate was analyzed. In this study, transects of 300 m in length were drawn, spaced 50 m apart. The Linear Regression Rate (LRR) method was applied. Vulnerability classes were assigned based on Pantusa et al. (2018), where a coastline change rate > 1.5 m/year corresponds to low vulnerability (1), between -0.5 and 1.5 m/year corresponds to moderate vulnerability (2), and < -0.5 m/year corresponds to high vulnerability (3).

- Land elevation (m)

The digital elevation model (DEM) from the TOPODATA/INPE database was used, based on the SRTM (Shuttle Radar Topography Mission) data with a spatial resolution of 30 m, scenes 15_405 and 15_39_. Classification followed Carvalho and Guerra (2020), where locations with elevation less than 5 m were considered as high vulnerability (3), between 5 and 8 m, moderate vulnerability (2), and greater than 8 m, low vulnerability (1).

- Beach morphodynamics (Ω) and slope (°)

Beach morphodynamics and slope were obtained from beach profile data collected by the beach monitoring research group at the Federal University of Southern Bahia (UFSB) between November 2018 and October 2019, at the sampling points shown in Figure 1. The face slope (tan β) was calculated using the arctangent function. The morphodynamic state was calculated using the formula by Kriebel et al. (1991): $\tan\beta = 0{,}15\ \Omega^{-1/2}$.

After calculating the slope and morphodynamics for each point, the data were interpolated using the Inverse Distance Weighted (IDW) method to generate raster data covering the entire study area. Subsequently, vulnerability classifications were assigned for both indicators. For slope, values greater than 6° were classified as low vulnerability (1), between 3° and 6°, as moderate vulnerability (2), and less than 3°, as high vulnerability (3). For morphodynamics, beaches were classified following Abuodha and Woodroffe (2006): dissipative beaches were assigned high vulnerability (3), intermediate beaches moderate vulnerability (2), and reflective beaches low vulnerability (1).

- Shoreline type

For this indicator, the shoreline type was classified using the nomenclature proposed by *Projeto Orla* (Brazil, 2006), considering the presence or absence of reefs and/or beachrock bordering the coastline through visual interpretation of satellite images. The classification also took into account the shoreline's exposure to waves from any direction that may directly or indirectly impact the coast. Protected beaches were assigned low vulnerability (1), semi-exposed beaches moderate vulnerability (2), and exposed beaches high vulnerability (3), based on Serafim and Bonetti (2017).

- Beach orientation (°)

The orientation of the coastline was identified using the compass tool in Google Earth Pro based on the transects generated in the coastline change rate analysis. Orientation data were generated as points vector files, and interpolation was performed in QGIS to produce a raster file covering the entire study area. Vulnerability classification was then applied, considering that coastlines facing the southern quadrant (120° to 225°) are more vulnerable, as they are exposed to higher-energy waves (Fernandino et al., 2019). Coastlines oriented to the east (67.5° to 120°), which receive the most frequent waves throughout the year, were classified as having moderate vulnerability. Those facing the northeast (45° to 67.5°), where wave energy is lower, were considered to have low vulnerability (Fernandino et al., 2019).

- Wave height (m)

The wave height indicator was based on the results found by Fernandino et al. (2019). The authors modeled the wave regime for the studied coast using data from the SMC-Brasil database. This system includes a global reanalysis dataset that provides hourly sea state data from 1948 to 2008, known as the Global Ocean Waves (GOW) database, which allows for the description of deep-water waves (Reguero et al., 2012 apud Fernandino et al., 2019). As a result, the authors found that the most frequent waves had average heights ranging from 1.0 to 1.5 meters. Therefore, in this study, this wave height range (1.0 to 1.5 m) was considered for the entire coastline and classified as moderate vulnerability (2), according to Carvalho and Guerra (2020).

- Presence of river mouths (m)

An analysis was conducted using satellite imagery to assess the rate of shoreline change to identify the migration areas of the river mouths within the study area (Figure 1). Based on this identification, the influence area was measured and classified accordingly: up to 50 m from the river mouth was considered high vulnerability (3), from 50 to 100 m moderate vulnerability (2), and beyond 100 m high vulnerability (3), following the criteria established by Sousa et al. (2013).

- Beach width (m)

For this parameter, cross-shore transects were drawn at 100-meter intervals from the reference shoreline described in the shoreline change rate section to the waterline. After this process, vulnerability was classified based on Ribeiro et al. (2013), where beach sections with a width greater than 30 meters were classified as low vulnerability (1), between 20 and 30 meters as moderate vulnerability (2), and less than 20 meters as high vulnerability (3).

- Occupation and vegetation **(**%)

Occupation and vegetation were obtained using the same method, through supervised classification of a CBERS-4A satellite image dated December 30, 2023, provided by the INPE (National Institute for Space Research) catalog. A subset of the image was extracted for the study area, followed by the creation of a color composition using bands 1, 2, 3, and 4. A pan-sharpening process was then applied using the Pansharpening tool in QGIS to enhance the spatial resolution from 8 meters to 2 meters.

Using the Dzetsaka plugin, supervised classification of the image was performed. Following this, the percentages of vegetation and land occupation were analyzed in segments of approximately 1,000 meters in length. Vulnerability was then classified, adapted from Sousa et al. (2013), considering that segments with more than 60% vegetation and less than 30% occupation were assigned low vulnerability (1); those with 30% to 60% for both indicators were considered to have moderate vulnerability (2); and segments with less than 60% vegetation and more than 30% occupation were classified as high vulnerability (3).

Tabela 1. Vulnerability classes for each indicator.

INDICATOR	**LOW**	**MODERATE**	**HIGH**
	1	**2**	**3**
Land Elevation (m)	> 8	5 a 8	< 5
Beach slope (º)	> 6	3 a 6	< 3
Beach morphodynamics	Reflective	Intermediate	Dissipative
Presence of river mouths (m)	>100	50 a 100	< 50
Beach width (°)	45 a 67,50	67,50 a 120	120 a 225
Shoreline type	Protected	Semi-exposed	Exposed

Beach width (m)	> 30	20 a 30	< 20
Vegetation (%)	> 60	30 a 60	< 30
Rate of coastline change (m/year)	> 1,5	0,5 a 1,5	< 0,5
Wave height (m)	< 0,5	0,5 a 1,5	> 1,5
Occupation (%)	< 30	30 a 60	> 60

3.2. Coastal Vulnerability Index (CVI)

- Conditions and scenarios

For the calculation of the Coastal Vulnerability Index, two conditions were evaluated under two possible scenarios. The first condition considers a current constant sea level (CSL) in relation to eustatic fluctuations. The second condition considers the most pessimistic projection of eustatic sea level rise (SLR) by the IPCC (2023) under a very high greenhouse gas emissions scenario (SSP5-8.5), with an increase of 0.20–0.29 m by 2050 and 0.63–1.01 m by 2100.

Regarding the scenarios, a moderate scenario (MS) was considered, assigning a vulnerability rating of 2, corresponding to the combination of spring tide/moderate rainfall (100 to 150 mm) or neap tide/cold front. The pessimistic scenario (PS), with a vulnerability rating of 3, accounted for the combination of spring tide/intense rainfall (< 300 mm)/cold front. These scenarios were configured considering moderate rainfall as the precipitation volume recorded in November and December 2022 in the cities of Porto Seguro and Santa Cruz Cabrália, and high rainfall as the extreme event on April 21, 2023, when the rainfall in Santa Cruz Cabrália exceeded 300 mm (Cemaden, 2024).

- Weighting of indicators and calculation of the Coastal Vulnerability Index (CVI)

The Analytic Hierarchy Process (AHP), developed by Saaty (1987), was used to weight the indicators. This method is frequently applied in coastal vulnerability studies (Gargiulo, Battarra; Tremiterra, 2020). It involves creating a pairwise comparison matrix between the variables, assigning a judgment value according to an importance scale ranging from 1 (equal importance) to 9 (extreme importance), as shown in Table 2. In this study, the conditions CSL and SLR were treated as indicators in the Coastal Vulnerability Index calculation. Since these conditions are associated with climate-oceanographic scenarios, they were assigned higher weights: a weight of 5 was assigned to SLC relative to all other indicators, and a weight of 7 to SLR.

Tabela 2. Saaty's Fundamental Scale of Importance Intensity (1977, 1987).

INTENSITY OF IMPORTANCE	DEFINITION	MEANING
1	Equal importance	Two activities contribute equally.
3	Moderate importance of one over the other	Experience and judgment slightly favor one activity over the other.
5	Strong or essential importance	Experience and judgment strongly favor one activity over the other.
7	Very strong importance	One activity is strongly favored over another; its dominance is demonstrated in practice.

9	Extreme importance	The evidence favoring one activity over another is of the highest possible order of affirmation.
2,4,6,8	Intermediate values between adjacent importance levels	When a compromise between two definitions is sought.
Principle of Reciprocity	When activity i is assigned one of the above importance levels when compared to j, then j will have the reciprocal value when compared to i.	A reasonable assumption.

To reduce the subjectivity of the pairwise comparison matrix evaluations, the consistency ratio (CR) was calculated, given by:

$$CR = \frac{CI}{RI}$$

Eq (1)

The CR for the two matrices were 0.081 and 0.093, respectively. Thus, the index calculation was carried out according to the flowchart below:

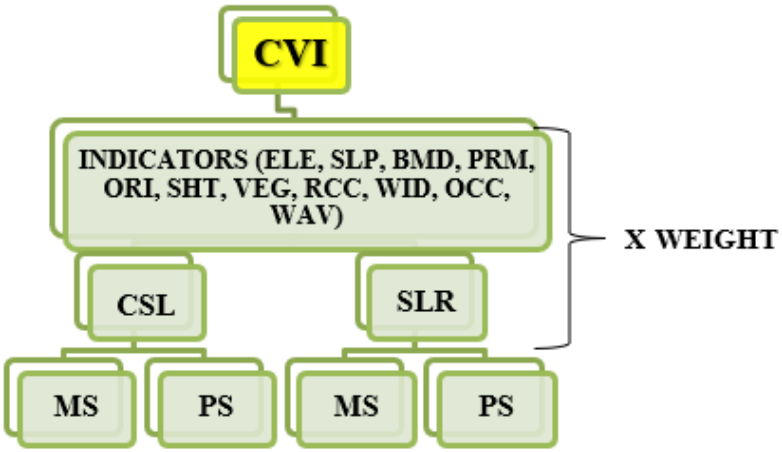

Figure 2. Organogram of the Coastal Vulnerability Index (CVI). Where: ELE – Land Elevation, SLP - Slope, BMD - Beach Morphodynamics, PRM - Presence of River Mouths, ORI - Orientation, SHT - Shoreline Type, VEG - Vegetation, RCC - Rate of coastline change, WID - Width, OCC - Occupation, WAV - Wave Height, CSL - Constant Sea Level, SLR -Eustatic sea level rise, MS - Moderate Scenario, PS - Pessimistic Scenario.

CVI = ELE * w + SLP * w + BMD * w + PRM * w + ORI * w + SHT * w + VEG * w + RCC * w + WID * w + OCC * w + WAV * w + CSL or SLR/MS or PS* w

w corresponds to the weight of each indicator

Eq. (2)

The CVI result, estimated for the CSL condition in the moderate scenario, was divided into three equal intervals within the GIS environment to determine low, moderate, and high vulnerability. The same intervals were applied to other conditions and scenarios. Thus, segments with values ≤ 1.91 were classified as low coastal vulnerability to erosion and flooding; values between 1.91 and 2.16 as moderate vulnerability; and values > 2.16 as high vulnerability.

4. Results

4.1. Vulnerability According to the Indicators

The results regarding terrain elevation suggest high vulnerability in 87.04% of the coastline and 12.96% moderate vulnerability, mostly concentrated on the beaches of Arraial d'Ajuda (Figure 3). The slope ranged from 2.06° at Mutá Beach – PS to 9.19° at Arakakaí Beach – SCC, with a mean and median of 6.35° and 6.45°, respectively. Vulnerability was classified as low for 69.77% of the coastline, moderate for 28.41%, and high for 1.48%.

Regarding morphodynamics, 21.99% of the coastline exhibited low vulnerability, classified as reflective beaches, mainly located in the central region of Santa Cruz Cabrália; 72.51% as moderate vulnerability (intermediate beaches), encompassing all beaches of Arraial d'Ajuda and the northern shore of Porto Seguro; and 5.50% as high vulnerability, corresponding to dissipative beaches located in the coastal arc of Mutá Beach (Figures 1 and 3).

The omega value ranged from 0.89 to 17.79, with an average of 6.35. Beach width varied from 91.70 m, located at the mouth of Rio dos Mangues, to 7.85 m at Ponta Grande Beach, with a mean of 28.02 m and a median of 26.10 m. Vulnerability for this indicator was low along 28.14% of the coast, moderate in 41.98%, and high in 40.69%, respectively.

The analysis of the coastline change rate generated 616 transects. The greatest retreat was 1.80 m/year at Ponta Grande Beach, while the greatest progradation was 2.28 m/year between Cruzeiro and Curuípe beaches (Figures 1 and 3) for the period from 2006 to 2023, with an average variation of 0.40 m/year. The results regarding vulnerability results indicated that 82.85% of the analyzed coastline has moderate vulnerability, 4.00% has low vulnerability and is in progradation, while 13.14% has high vulnerability and is in an erosive state, mainly concentrated at Ponta Grande Beach.

Ten river mouths were identified along the ~25 km of coastline (Figure 1). Based on this parameter, 83.74% of the coast was classified as low vulnerability, 7.46% as moderate, and 8.97% as high. Regarding beach orientation, 6.18% of the coast has low vulnerability, 84.81% moderate, and 9.01% high vulnerability, respectively. The analysis of the shoreline type relative to the presence of reefs showed that 32.08% of the coastline is sheltered, classified as low vulnerability, 20.61% as moderate vulnerability, while 47.31% of the beaches are exposed, with high vulnerability to erosion and flooding.

The vegetation indicator showed that 6.24% of the area has low vulnerability, 63.64% moderate vulnerability, and 30.12% high vulnerability. Coastal occupation indicated low vulnerability of 11.68%, and 47.63% and 40.69% for moderate and high vulnerability, respectively. Regarding waves, the entire studied coastline was classified as moderate vulnerability.

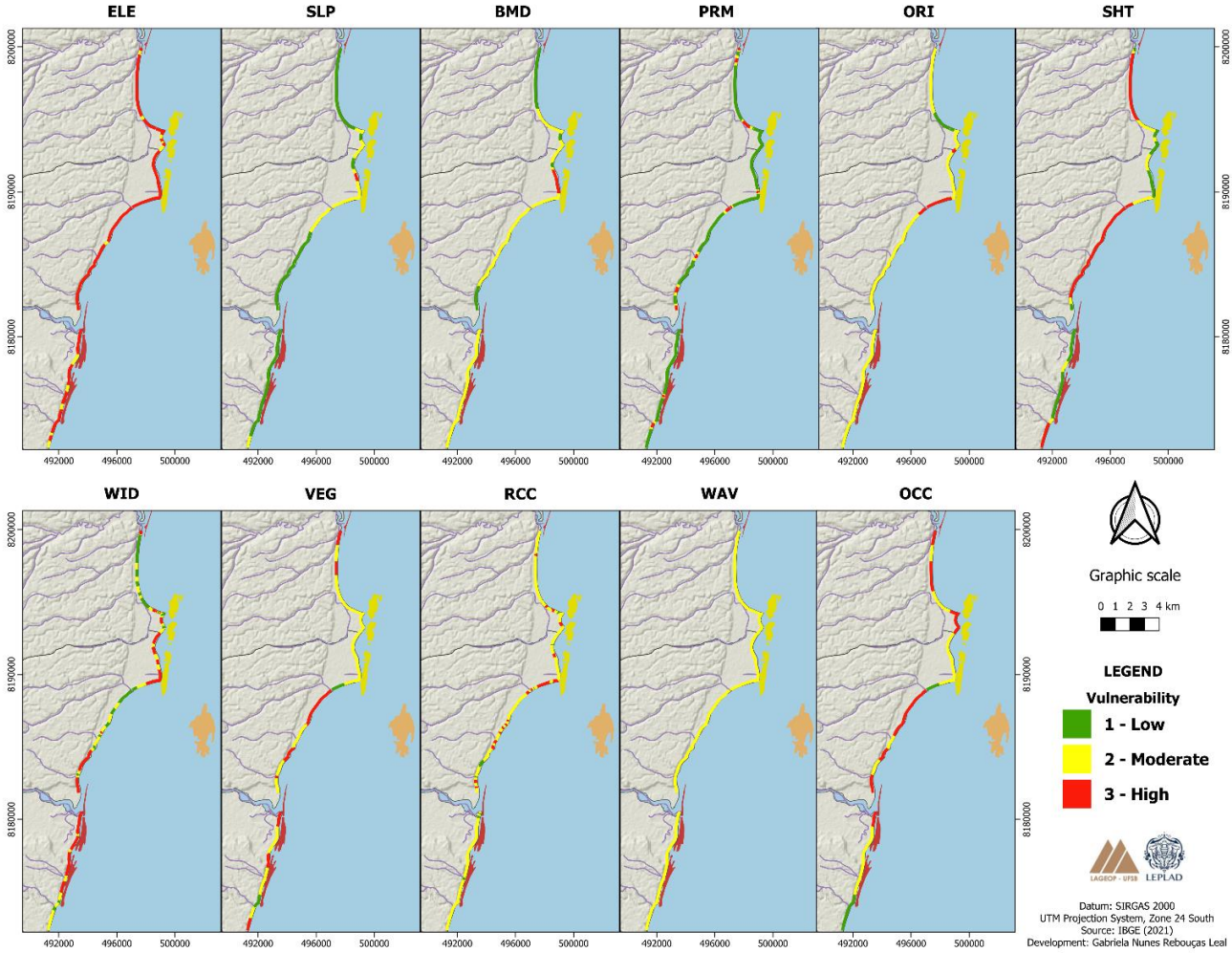

Figure 3. Coastal vulnerability map by indicator of the study area. ELE - land elevation, SLP - slope, BMD - Beach Morphodynamics, PRM - Presence of River Mouths, ORI - Orientation, SHT - Shoreline Type, WID – Width, VEG - Vegetation, RCC - Rate of coastline change, WAV - Wave Height OCC - Occupation, According to the classes in Table 1.

4.2. Coastal Vulnerability Index (CVI) – Conditions and Scenarios

The results of the CVI under the moderate scenario with the condition of constant mean sea level (CSL – MS) indicated that 12.90% of the coastline was classified as having low vulnerability, 59.77% as moderate vulnerability, and 27.33% as high vulnerability (Figure 4), with concentrations in the Northern Shoreline (PS) and Ponta Grande Beach (PS). Under the condition of eustatic sea level rise within the same scenario (SRL – MS), vulnerability was low along 6.30% of the coast, moderate along 57.92%, and high along 35.78%.

When the CVI was calculated under both conditions (CSL and SLR) in a scenario with a cold front, spring tide, and storm surge (CP), the coastline showed no areas with low vulnerability, and there was a significant increase in areas with high vulnerability to erosion and flooding. Under the CSL condition, 80.95% of the coast was classified as having high vulnerability, and under the SLR condition, this percentage rose to 98.48%.

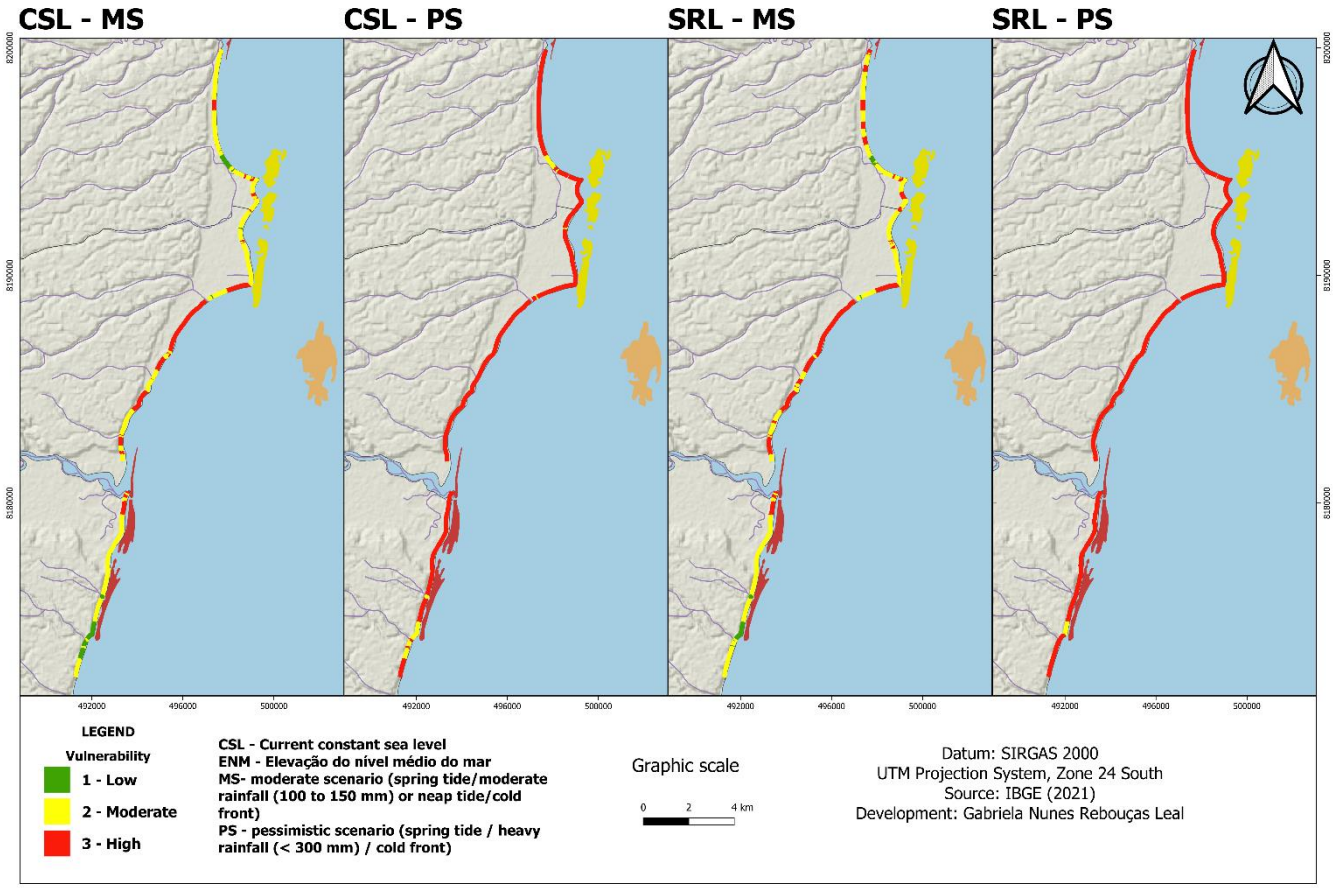

Figure 4. Map of the Coastal Vulnerability Index under the conditions of CSL (Current constant sea level) and SLR (eustatic sea level rise) in a moderate scenario (MS) and a pessimistic scenario (PS).

5. Discussion

This study assessed coastal vulnerability, encompassing physical, environmental, and socioeconomic factors. The set of indicators used to compose the index analyzed the specificities of the location, which Bonetti and Woodroffe (2017) consider the best alternative, although this approach is limited in its comparison with other locations.

The results for slope and beach morphodynamics, generated from field data, allowed for a consistent spatial representation. These indicators are interrelated, as dissipative beaches are characterized by flat and gentle profiles, while intermediate and reflective beaches tend to have steeper profiles (Calliari, 2003; Barros; Wasserman, 2022). Slope conditions indicated low vulnerability for most of the study area, associated with intermediate and reflective beaches.

Regarding shoreline variation, Ponta Grande Beach was the area with the highest concentration of erosive segments, where the erosion has damaged the BR-367 highway infrastructure, disturbing the population since it is the main access route between the municipalities of Porto Seguro and Santa Cruz Cabrália. This phenomenon occurs due to a combination of regional wave climate characteristics—SSE waves undergo intense diffraction at Recife do Fora and reach the coast with greater energy—together with the beach's south-facing orientation and the presence of the rigid BR-367 structure (Fernandino et al., 2019).

Due to intense urbanization, greater vulnerability was observed in the Northern Shore (PS), the central area of Porto Seguro, and at the Coroa Vermelha Beach (SCC). The expansion of coastal occupation is considered the main driver of restinga vegetation suppression (França; Gomes, 2022; Carvalho et al., 2018). The results for vulnerability regarding these indicators (occupation and vegetation) show a clear relationship: areas with high occupation rates exhibited low vegetation cover.

Beach width showed less vulnerable segments along the beaches of Santa Cruz Cabrália, where development is farther from the sea, allowing the sandy beach to grow during accretion phases (fair weather/summer) and re-accommodate eroded sediments during erosive periods (cold fronts/winter), despite the shoreline is also urbanized. In contrast, at Coroa Vermelha, Mutá, Ponta Grande, and Arraial d'Ajuda beaches, the presence of reefs bordering the coast and urban structures close to the sea reduce the beach width. Thus, during high tide, access becomes limited, preventing the passage of people and the recreational use. Furthermore, the narrow beach width associated with coastal urbanization can interfere with the natural wave mobility process and alter sediment dynamics patterns, as these areas lack the necessary space for wave accommodation, making them more vulnerable to erosive processes (Barros; Wasserman, 2022).

On the Northern Shore of Porto Seguro, the least vulnerable segment in terms of beach width is associated with the mouth of the Rio dos Mangues, which showed the highest mobility along the coastline, shifting about 600 meters southward. The migration of river mouths can modify the longshore drift patterns in associated beach segments, especially when river flow is stronger than the drift, intensifying sediment accumulation updrift and severe erosion downdrift (Souza et al., 2005; Marino et al., 2016). In the case of Rio dos Mangues, damage to structures is observed where the river shifts course, with sandbags being used for protection, while on the updrift side, the presence of mangroves and the absence of urban occupation keep the beach more preserved.

It is important to note that the lack of recent and detailed wave data for the study area limited a more in-depth analysis of this indicator. The same issue occurred with the terrain elevation indicator, where the low spatial resolution of the Digital Elevation Model (DEM) may have produced more generalized results regarding the area's altimetry. In this context, efforts toward the generation of high-quality local data are essential.

5.1. Coastal Vulnerability Index (CVI) – Conditions and Scenarios

The CVI results indicated that the tide and rainfall/cold front scenario (PS) is more decisive for coastal vulnerability than the eustatic rise in mean sea level. When observing the moderate and pessimistic scenarios under the CSL condition, the increase in high vulnerability sectors was 53.68%, and under the SLR condition, it was 62.70%. These factors indicate that understanding the effects of cold front weather events on storm tides is just as necessary as projecting the consequences of future sea level rise, as the impacts of these phenomena are already being observed in the region's coastal zone.

In recent years, several events have illustrated the scenarios described above: i) the tropical storm that occurred in early December 2018 (Figure 5), where strong winds and heavy rainfall caused flooding and damaged commercial structures in the region (Sul Bahia News, 2018); ii) Tropical Storm IBA (a Tupi-Guarani term meaning "bad"), which caused rough seas and strong winds along the coast in 2019 (G1, 2019); and iii) the heavy rainfall that hit the region in April 2019, especially in the city of Santa Cruz Cabrália, where approximately 400 mm of rain fell in a single day (April 21, 2019), leading to river overflow—particularly the Yaya River—flooding the entire lower part of the city and breaking through the coastal barrier that channels its flow northward to the river mouth (Figure 5). On that occasion, a state of emergency was declared in the affected municipalities, and about 4,000 people were left homeless.

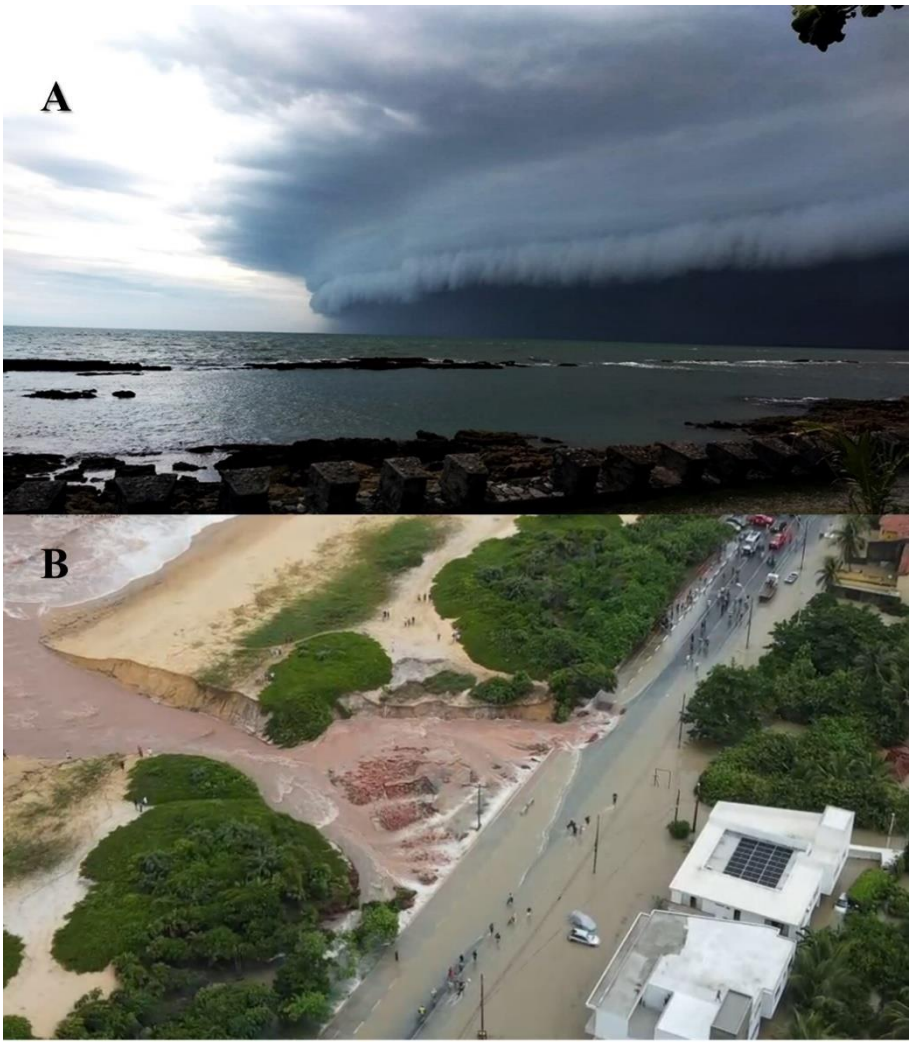

Figure 5. A - Tropical storm in 2018. Source: Sul Bahia News (2018). B - Erosion and flooding in Santa Cruz Cabrália in April 2023, with the breach of the Yaya River coastal barrier. Source: Belmonte News (2023).

These events occurred with the arrival of cold fronts associated with spring tides (DHN 2018/2019/2020), factors that intensify coastal vulnerability, as the flood level remains elevated for a longer period, hindering river drainage, and allowing waves to reach the shore with greater intensity (Gouvea Jr; Fernandes; Castro, 2022). It is worth noting that, under extreme rainfall scenarios, combined with meteorological and astronomical tides, nearly the entire coastal zone shows a high degree of vulnerability under both analyzed conditions — even in beaches bordered by reefs or beach sandstones. This is because during astronomical tides, along with the passage of cold fronts, the seasonal rise in sea level surpasses the height of these ecosystems, allowing waves to directly impact the shoreline.

With the eustatic rise in mean sea level, it is expected that high vulnerability will become permanent, as the water column depth increases, leaving reefs and sandstone beds submerged for longer periods. Consequently, their capacity to dissipate wave energy will be reduced, exposing beaches and placing habitats, coastal structures, and biodiversity at risk. This directly affects the region's economy, which relies heavily on these natural resources (Ferrario et al., 2014; Sigle; Costa, 2017; Summers et al., 2018; Elliff et al., 2019).

Coastal occupation was considered the most significant indicator in the Coastal Vulnerability Index, similarly to the findings of Marino et al. (2016) in beaches of Ceará, and Hzami et al. (2021) in North Africa. However, although the method yielded important results, it is necessary to acknowledge the subjectivity in the selection of indicators and the definition of vulnerability ranges — aspects that must be carefully considered when interpreting the analyses.

Another important point is that neither of the studied municipalities has a municipal coastal management plan, an essential tool for establishing coastal use guidelines aimed at preserving its resources (Bahia, 2018). Studies by CI (2013) project a temperature increase of 2.1 °C for Santa Cruz Cabrália and 2.3 °C for Porto Seguro, Bahia, by 2050. With an estimated sea level rise of 50 cm, ~58 million dollars invested by the hotel sector may be at risk, as many hotels are located between 10 and 60 meters from the coastline (CI, 2013).

Managing an area of multiple interests — cultural, economic, environmental, and political — is challenging. Moreover, public authorities must consider the impacts of climate change and the goals established by the UN's 2030 Agenda. In this sense, the data generated in this study may contribute to setting priorities for planning prevention and adaptation measures in the coastal zone of the region.

Developing strategies to address climate change, with a focus on coastal protection, should be a priority in municipal action plans. It is essential to promote environmental monitoring programs that enable the collection of data to assess vulnerabilities and adequately plan the use and occupation of coastal areas. Additionally, it is necessary to ensure compliance with regulations related to Permanent Preservation Areas (APPs) and, when necessary, to establish conservation units on uninhabited coastal lands, aiming to facilitate the recovery of restinga vegetation and strengthen its role in sediment retention. It is also worth considering the relocation and/or removal of facilities located in areas of mouth mobility, as these areas are vulnerable to both erosion and flooding.

6. Conclusions

Overall, the CVI yielded relevant results, especially by demonstrating that the combination of cold fronts, rainfall, and spring and meteorological tides renders the coastal zone highly vulnerable—an effect already observed during recent extreme events in the region. With the onset of eustatic sea level rise, these challenges are expected to intensify, impacting shoreline occupation patterns. In this context, adaptation strategies should be prioritized within a coastal management plan that considers the various stakeholders involved in the political, environmental, and social spheres.

The weighting process using the AHP method aimed to assign quantitative importance values to each indicator and condition analyzed. The most influential indicators in determining coastal vulnerability were land occupation, shoreline change rate, beach orientation, and beach width. It is important to highlight that the method contains certain subjectivities, particularly regarding the selection of indicators and the assignment of vulnerability levels. Nevertheless, the final product—the calculated index—yielded consistent results, showing high vulnerability in locations already experiencing visible erosion and flooding impacts.

Some challenges were encountered during the development of this study, including the lack of updated wave data, detailed data on floating population (especially by neighborhood), and the absence of a high-radiometric-resolution Digital Elevation Model (DEM). Based on this, it is essential to implement an oceanographic buoy, enhance continuous beach monitoring efforts, to promote the collection and spatialization of socioeconomic data, high-resolution remote sensing imagery, floating population data, and coastal carrying capacity assessments.

As the region stands out in national tourism due to its rich natural ecosystems, this study may serve as a reference for coastal management projects by public and/or private entities—particularly with regard to erosion and flooding. Segments classified as having high vulnerability even under a moderate scenario, such as Ponta Grande Beach (PS), Northern Shore beaches (PS), and river mouths, should be prioritized for conservation/adaptation measures. These may include the relocation of coastal infrastructure such as the BR-367 highway. Additionally, other indicators may be incorporated into the index, such as river discharge data, beach water quality, algal bloom occurrences, as well as other types of vulnerability assessments, including the effects of cold fronts and sea level rise on coastal ecosystems and biodiversity.

Authors' Contributions: Conceptualization and methodology: G.N.; C.M.; T.P. Software, validation, formal analysis, investigation, data curation, and writing—original draft preparation: G.N. Review and supervision: C.M. and T.P. All authors have read and agreed to the published version of the manuscript.

Funding: This research was funded by the Fundação de Amparo à Pesquisa do Estado da Bahia – Fapesb, through a master's scholarship, grant number 4884, scholarship award term number 00061465910.

Acknowledgments: We thank the reviewers of this article for their contributions, the Programa de Pós-graduação em Ciências e Tecnologias Ambientais (UFSB/IFBA) and the Fundação de Amparo à Pesquisa do Estado da Bahia (FAPESB) for granting the scholarship.

Conflict of Interest: The authors declare no conflict of interest. The funders had no role in the study design; in the collection, analysis, or interpretation of data; in the writing of the manuscript; or in the decision to publish the results.

References

1. ABUODHA, P. A.O.; WOODROFFE, C. D. Assessing vulnerability to sea-level rise using a coastal sensitivity index: a case study from southeast Australia. **Journal of coastal conservation**, v. 14, p. 189-205, 2010. DOI: 10.1007/s11852-010-0097-0
2. AMARO, V. E. et al. Análise de Índices de Vulnerabilidade Física com uso de Geotecnologias na Região da Barreira do Inferno/RN. **Revista de Geociências do Nordeste**, p. 179-192, 2021. DOI: 10.21680/2447-3359.2021v7n2ID22034
3. BAIG, M. R. I. et al. Coastal vulnerability mapping by integrating geospatial techniques and analytical hierarchy process (AHP) along the Vishakhapatnam coastal tract, Andhra Pradesh, India. **Journal of the Indian Society of Remote Sensing**, v. 49, p. 215-231, 2021. DOI: 10.1007/s12524-020-01204-6
4. BARROS; WESSERMAN. A evolução dos usos das praias e seus conceitos. IN: BOMBANA, Briana, TURRA, Alexandra; POLETTE, Marcus (Org.). **Gestão de praias: do conceito à prática**. São Paulo: Instituto de Estudos Avançados da Universidade de São Paulo, 2022.
5. BRASIL. 2016. Ministério do Turismo. **Bahia tem novo mapa do turismo**. Disponível em: <http://www.turismo.gov.br/%C3%BAltimas-not%C3%ADcias/6466-bahia-tem-novo-mapa-tur%C3%ADstico.html>. Acesso em: 05/05/**2024**
6. BONETTI, J. E.; WOODROFFE, C. D. Spatial Analysis on GIS for Coastal Vulnerability Assessment. In: BARTLETT, D. and CELLIERS, L. (eds.). **Geoinformatics for Marine and Coastal Management**. Cap. 16. CRC Press, Boca Raton, p. 367-396, 2017.
7. BUSH, D. M. et al. Utilization of geoindicators for rapid assessment of coastal-hazard risk and mitigation. **Ocean and Coastal Management**, v. 42, n. 8, p. 647-670, 1999.DOI: 10.1016/S0964-5691(99)00027-7
8. BOAK, E. H.; TURNER, I. L. Shoreline Definition and Detection: A Review. **Journal of Coastal Research**, v.21, n.4, p. 688–703, 2005. ISSN 0749-0208.
9. BUSMAN, D. V.; AMARO, V. E.; SOUZA FILHO, P. W. M. Análise estatística multivariada de métodos de vulnerabilidade física em zonas costeiras tropicais. **Revista Brasileira De Geomorfologia**, vol. 17, 2016. DOI: 10.20502/rbg.v17i3.912
10. CALLIARI, L. J. et al. Morfodinâmica praial: uma breve revisão. **Revista brasileira de oceanografia**, v. 51, p. 63-78, 2003. DOI:10.1590/S1679-87592003000100007
11. CARVALHO, B. C.; GUERRA, J. V. Coastal vulnerability of Rio de Janeiro shoreline (SE Brazil) due to natural and social impacts**. Journal of Coastal Research**, v. 95, p. 759-763, 2020. DOI: 10.2112/SI95-148.1
12. CARVALHO, R. C. O de; PIMENTA, F. de S.; SCHIAVETTI, A. Museu aberto do descobrimento (MADE) na Bahia, Brasil: geossistema e vulnerabilidade ambiental. **Gaia Scientia**, v. 12, n. 4, p. 16-32, 2018. DOI:10.22478/ufpb.1981-1268.2018v12n4.34093
13. ELLIFF, C. I. et al. Wave attenuation and shoreline protection by a fringing reef system. **Anuário do Instituto de Geociências - UFRJ**, v. 42, n. 1, p. 87-94, 2019.
14. FRANÇA, J.; GOMES, I. E. Orla Marítima em Regiões de Grande Especulação Imobiliária no Extremo Sul da Bahia: Caracterização de Mudanças No Uso de Solo e Mapeamento de Acessos Públicos Às Praias. **Costas**, v. 4, n. 1, p. 59-70, 2022. DOI:10.25267/Costas.2023.v.3.i2.04
15. FERNANDINO, G. et al. Erosional patterns induced by coral reefs in the eastern coast of Brazil. **Pesquisas em Geociências**, v. 45, 2019. DOI:10.22456/1807-9806.91391

16. FERRARIO, F. et al. The effectiveness of coral reefs for coastal hazard risk reduction and adaptation. **Nature communications**, v. 5, n. 1, p. 1-9, 2014. DOI:10.1038/ncomms4794
17. FILGUEIRAS, G. D. L.; ALBINO, J. Vulnerabilidade costeira a partir da abordagem multicritério: estudo de caso no litoral sul do Espírito Santo. **Revista do Departamento de Geografia**, v.40, p. 78-93, 2020. DOI: 10.11606/rdg.v40i0.165831
18. FIRTH, L. B. et al. Ocean sprawl: challenges and opportunities for biodiversity management in a changing world. In: DALE, A. C.; SMITH, I. P.; HUGHES, R. N.; HUGHES, D. J. (Eds.). **Oceanography and Marine Biology:** An Annual Review. Boca Raton: CRC Press, p. 193–269, 2016.
19. GARGIULO, C.; BATTARRA, R.; TREMITERRA, M. R. Coastal areas and climate change: A decision support tool for implementing adaptation measures. **Land Use Policy**, v. 91, p. 104413, 2020. DOI: 10.1016/j.landusepol.2019.104413
20. GRACIA PRIETO, F. J. The complexity of studying coasts: From forms and processes to management. **Cuadernos de Investigación Geográfica**, Logroño, SPA, v. 48, n. 2, p. 219–255, 2022. DOI: 10.18172/cig.5451
21. GORNITZ, V. Global coastal hazards from future sea level rise. Palaeogeography, Palaeoclimatology, **Palaeoecology**, v. 89, n. 4, p. 379-398, 1991. DOI: 10.1016/0031-0182(91)90173-O
22. GOUVEA JR, W. C.; FERNANDES, D.; CASTRO, J. W. de A. Análise das variáveis físicas e dinâmicas do Índice de Vulnerabilidade Costeira (IVC) na enseada da Baia Formosa, Região dos Lagos Fluminense, Estado do Rio de Janeiro. **Revista Brasileira de Geomorfologia**, v. 23, n. 4, p. 1812-1833, 2022. DOI: 10.20502/rgb.v23i4.2144
23. HZAMI, A. et al. Alarming coastal vulnerability of the deltaic and sandy beaches of North Africa. **Scientific reports**, v. 11, n. 1, p. 2320, 2021. DOI:10.1038/s41598-020-77926-x
24. IBGE – INSTITUTO BRASILEIRO DE GEOGRAFIA E ESTATÍSTICA. **Censo Brasileiro de 2022**. Rio de Janeiro: IBGE, 2022. Disponível em: < <https://cidades.ibge.gov.br/brasil/ba/porto-seguro/panorama>. Acesso em: 30/11/2023
25. IBGE – INSTITUTO BRASILEIRO DE GEOGRAFIA E ESTATÍSTICA. **Censo Brasileiro de 2022**. Rio de Janeiro: IBGE, 2022. Disponível em: < https://cidades.ibge.gov.br/brasil/ba/santa-cruz-cabralia/panorama>. Acesso em: 30/11/2023
26. LUIJENDIJK, A. et al. The state of the world's beaches. **Scientific reports**, v. 8, n. 1, p. 1-11, 2018. DOI:10.1038/s41598-018-24630-6
27. KLEIN, A. H. da F. Um método indireto para a determinação do estágio morfodinâmico de praias oceânicas arenosas. In: C**ongresso da Associação Brasileira de Estudos do Quaternário**. p. 76-78, 1997.
28. MARINO, M. T. R. D. et al. Vulnerabilidade física de parte do litoral leste do Ceará à erosão. **Desenvolvimento e Meio Ambiente**, Curitiba, v. 38, p. 253-281, 2016. DOI:10.5914/tropocean.v38i2.5167
29. MENTASCHI, L. et al. Global long-term observations of coastal erosion and accretion. **Scientific reports**, v. 8, n. 1, p. 12876, 2018. DOI:10.1038/s41598-018-30904-w
30. PANTUSA, D. et al. Application of a coastal vulnerability index. A case study along the Apulian Coastline, Italy. **Water**, v. 10, n. 9, p. 1218, 2018. DOI:10.3390/w10091218
31. QUEIROZ, H. A. de A.; GONÇALVES, R. M.; MISHRA, M. Characterizing global satellite-based indicators for coastal vulnerability to erosion management as exemplified by a regional level analysis from Northeast Brazil. **Science of the Total Environment**, v. 817, p. 152849, 2022. DOI: 10.1016/j.scitotenv.2021.152849
32. RUEDA, A. et al. A global classification of coastal flood hazard climates associated with large-scale oceanographic forcing. **Scientific Reports**, v. 7, n. 1, p. 1-8, 2017. DOI:10.1038/s41598-017-05090-w

33. SEI - Superintendência de Estudos Econômicos e Sociais da Bahia. **Boletim de atividades características do turismo da Bahia**, Salvador, v. 4, 2022. Disponível em: < http://www.observatorio.turismo.ba.gov.br/wp-content/uploads/2023/05/bactba_2022.pdf >. Acesso em: 20/04/2024.
34. SAATY, R. W. The analytic hierarchy process—what it is and how it is used. **Mathematical modelling**, v. 9, n. 3-5, p. 161-176, 1987. DOI: 10.1016/0270-0255(87)90473-8
35. SERAFIM, M. B.; BONETTI, J. Vulnerabilidade das praias do Estado de Santa Catarina a eventos de erosão e inundação costeira: proposta metodológica baseada em um índice multicritério. **Quaternary and Environmental Geosciences**, v. 8, n. 2, p. 36-54, 2017. DOI:10.5380/abequa.v8i2.47281
36. SILVA, I. R. et al. Potencial de danos econômicos face à erosão costeira, relativo às Praias da Costa do Descobrimento–Litoral Sul do estado da Bahia. **Pesquisas em Geociências**, v. 34, n. 1, p. 35-44, 2007. DOI: 10.22456/1807-9806.19461
37. SILVA, I. R. Subsídios para a gestão ambiental das praias da Costa do Descobrimento, litoral Sul do estado da Bahia, Brasil. **Revista de Gestão Costeira Integrada-Journal of Integrated Coastal Zone Management**, v. 8, n. 2, p. 47-60, 2008. DOI:10.5894/rgci135
38. SIEGLE, E.; COSTA, M. B. Nearshore wave power increase of reef-shaped costal due to sea-level rise. **Earth's Future**, v. 5, n. 10, p. 1054-1065, 2017. DOI:10.1002/2017EF000624
39. SILVA, I.R. Ambientes Costeiros. In: Silva, A.J.C.L.P. *et al* (Orgs). **Ambientes de sedimentação siliciclástica do Brasil**. São Paulo: Beca-BALL Ed, p.212-223, 2008.
40. SOUSA, P.H.G.O.; SIEGLE, E.T.M.G.; TESSLER, M.G. Vulnerability assessment of Massaguaçú Beach (SE Brazil). **Ocean and Coastal Management**, v. 77, p. 24-30, 2013.
41. SUMMERS, A. et al. Failure to protect beaches under slowly rising sea level. **Climatic Change**, v. 151, n. 1, p. 427-443, 2018. DOI: 10.1007/s10584-018-2327-7
42. ZANETTI, V. B.; SOUSA JR, W. C de; FREITAS, D. M de. A climate change vulnerability index and case study in a Brazilian coastal city. **Sustainability**, v. 8, n. 8, p. 811, 2016. DOI:10.3390/su8080811